

Supporting information

Polypyrrole-modified PVDF-HFP coaxial electrospun composite membranes for intelligent thermal management and electromagnetic interference shielding

Rongjun Wei^{a,b,c}, Bingqing Quan^{a,b,c}, Muyi Han^d, Xinpeng Hu^{a,b,c,*} and Xiang Lu^{a,b,c,*}

^aKey Laboratory of Material Chemistry for Energy Conversion and Storage, Huazhong University of Science and Technology, Ministry of Education, Wuhan 430074, China;

^bHubei Engineering Research Center for Biomaterials and Medical Protective Materials, Huazhong University of Science and Technology, Wuhan 430074, China;

^cHubei Key Laboratory of Material Chemistry and Service Failure, School of Chemistry and Chemical Engineering, Huazhong University of Science and Technology, Wuhan 430074, China;

^dDepartment of Materials Science and Engineering, National University of Singapore, Singapore 117575, Singapore

* Corresponding authors (emails: hxpbest@outlook.com (Xinpeng Hu);

luxiang@hust.edu.cn & luxiang_1028@163.com (Xiang Lu))

Experimental Section

Materials preparation:

Paraffin wax (PW), with melting point ranging from 36~39 °C, was purchased from Hangzhou Ruhr Technology Co., Ltd., China. Poly(vinylidene fluoride-hexafluoropropylene) (PVDF-HFP) was obtained from Shanghai Aladdin Bio-Chem Technology Co., Ltd. Pyrrole (C₄H₅N, AR) was procured from Shanghai E-En Chemical Technology Co., Ltd. Ferric chloride hexahydrate (FeCl₃ • 6H₂O, AR, 99%) was procured from Shanghai Jizhi Biochemical Technology Co., Ltd. Sodium dodecylbenzenesulfonate (C₁₈H₂₉NaO₃S, AR) and Anhydrous ethanol were both purchased from Sinopharm Chemical Reagent Co., Ltd.

Fabrication of PVDF-PW@PPy composite film

The PVDF-PW fiber membrane was fabricated via coaxial electrospinning using PW as the core material and PVDF-HFP as the shell material, with a mass ratio of 1:1. The extrusion flow rate of the core layer was maintained at 0.3 mL/h. The resulting fiber membranes displayed hydrophobic characteristics. Two separate solutions were prepared in an ice-water bath. Solution A was formulated by dissolving 1.4 mL of pyrrole and 0.2 g of C₁₈H₂₉NaO₃S in 100 mL of distilled water, while Solution B consisted of 5.4 g of FeCl₃ • 6H₂O dissolved in 100 mL of distilled water. Each solution was mechanically stirred for 1 hour. To deposit PPy onto the fiber membrane, the PVDF-PW substrate was initially wetted with ethanol and rinsed with deionized water. It was then immersed in Solution A for 20 minutes, after which Solution B was added dropwise to the mixture over a period of 5 minutes. The polymerization of PPy

was carried out for a total of 3 hours. Finally, the membrane was rinsed, subjected to post-treatment, and vacuum-dried at 50 °C to obtain the PVDF-PW@PPy composite membrane.

Characterization

The microstructure and surface element distribution of PVDF-PW and PVDF-PW@PPy composite membranes were observed using a field emission scanning electron microscope (FE-SEM, Hitachi SU8010) equipped with energy dispersive spectroscopy (EDS) at an acceleration voltage of 5 kV. The samples were sprayed with Au before observation. Chemical structures were determined by Fourier transform infrared spectroscopy (FTIR, Vertex 70) in the wavelength range of 600-4000 cm^{-1} . The crystal structure was tested by X-ray diffraction (XRD, Rigaku SmartLab-SE) using Cu-K α radiation at room temperature with a scanning rate of 10 °/min. The surface functional group structure was detected using X-ray photoelectron spectroscopy (XPS, Thermo Scientific ESCALAB Xi+). The phase change characteristics were detected by a differential scanning calorimeter (DSC25, TA) in the range of 0-60 °C, with a heating and cooling rate of 5 °C/min. Thermal stability was characterised using a thermogravimetric analyser (TGA55, TA) within 30-600 °C, with a temperature ramp rate of 10 °C/min under N₂ atmosphere. The reflectance (R) and transmittance (T) of PVDF-PW and PVDF-PW@PPy membranes were measured using a UV-Vis-NIR spectrophotometer (UV-3600). The Joule heating performance of the composite film was studied using a self-made circuit device, and the output voltage was obtained from a DC power supply (MS-305DS). The

photothermal conversion performance of composite films under different light intensities was evaluated using a simulated Xenon lamp. The real-time temperatures of the PVDF-PW@PPy composite film during electrical-to-thermal conversion and photothermal conversion tests were recorded by an infrared camera (FLIR, ThermaCAM SC3000). The EMI shielding performance was measured through coaxial measurement using Agilent N5247A vector network analyser in the X-band frequency range (8.2-12.4 GHz).

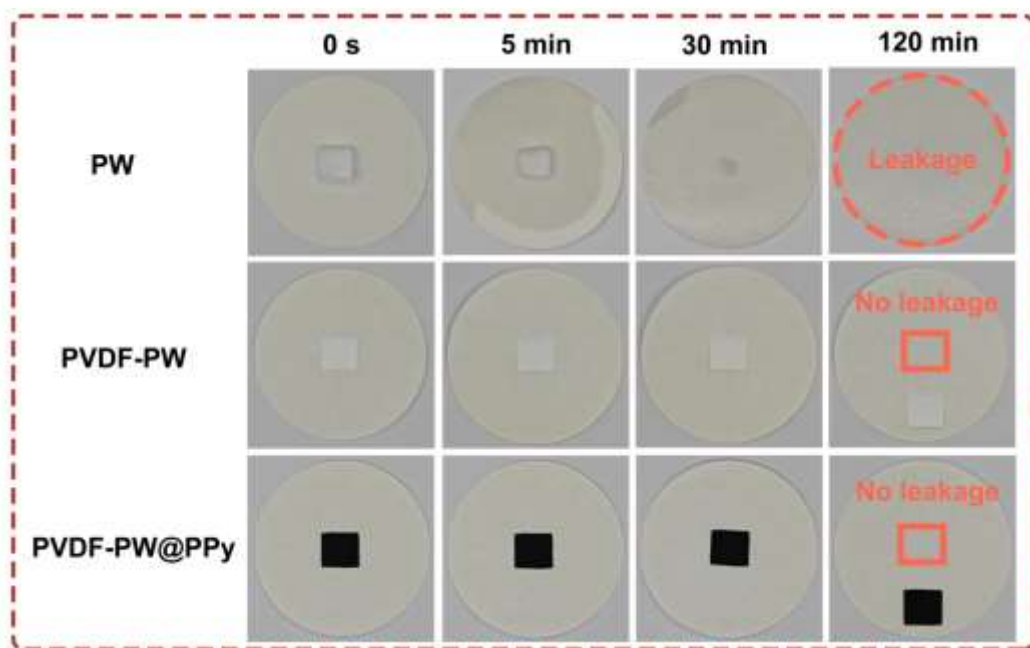


Figure S1 Anti-leakage test of the samples at 70 °C.

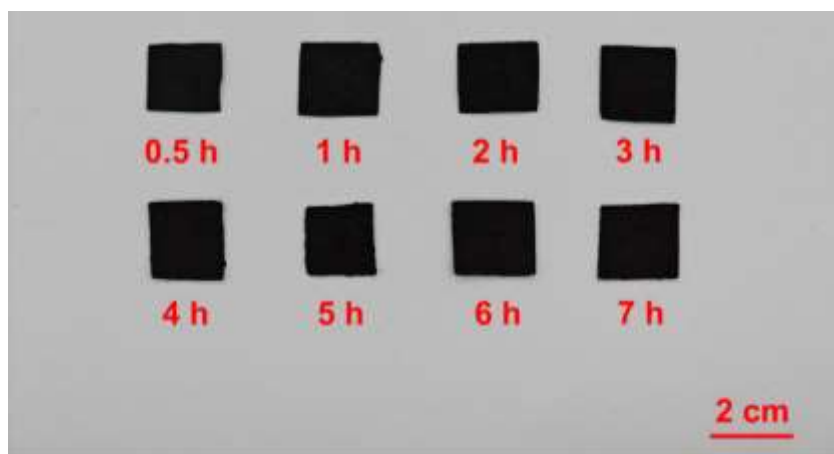


Figure S2 PVDF-PW@PPy composite films obtained at different polymerisation times.

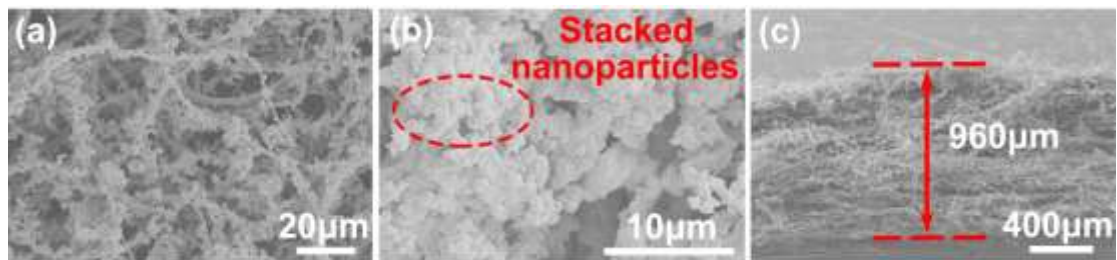


Figure S3 SEM images of composite films. (a) PPy polymerisation time of 2h. (b) PPy polymerisation time of 6h. (c) SEM image of thickness profile for PVDF-PW@PPy.

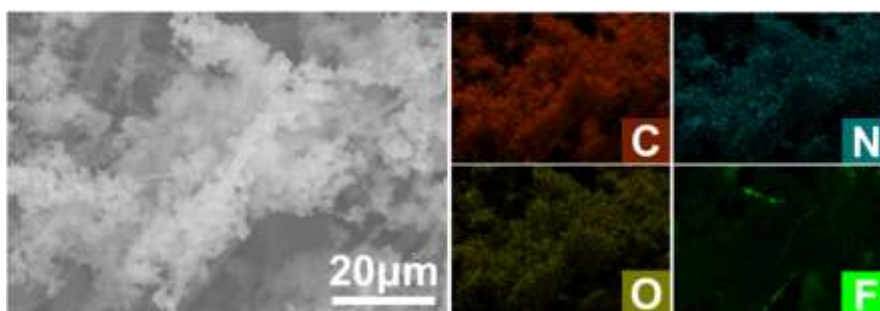


Figure S4 EDS images of PVDF-PW@PPy.

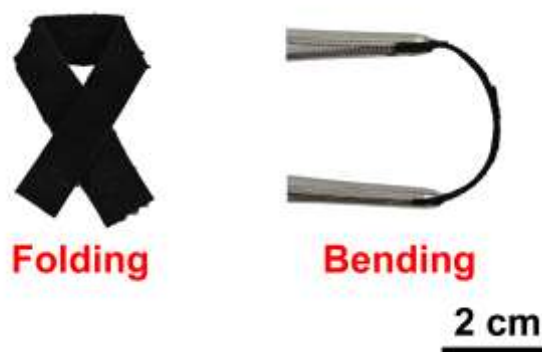


Figure S5 Images of PVDF-PW@PPy being folded and bent without damage.

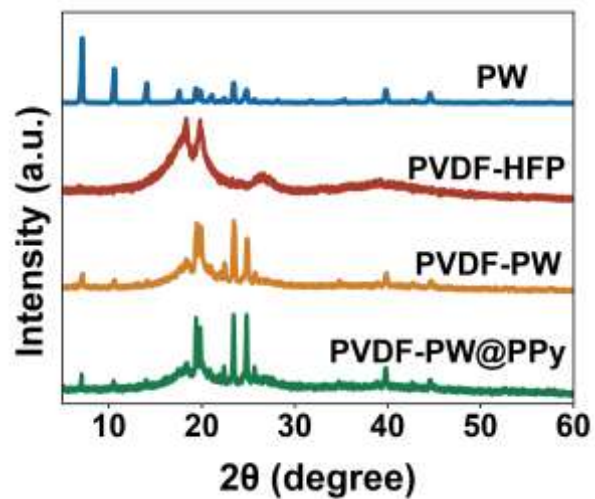


Figure S6 XRD pattern of the samples.

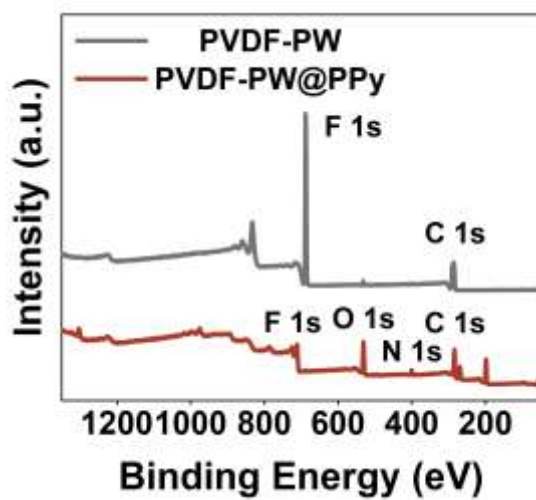


Figure S7 XPS curves of the samples.

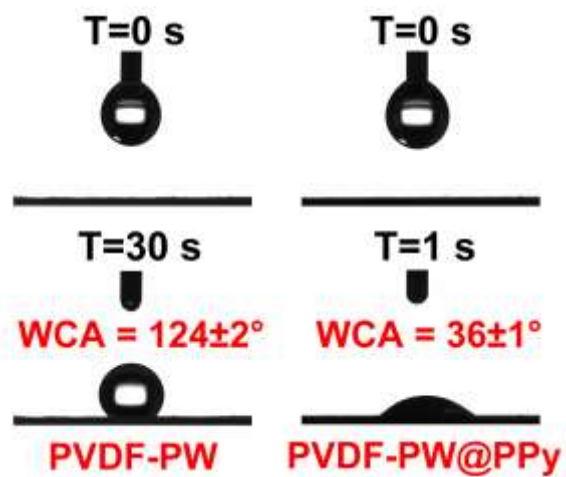


Figure S8 Water contact angle (WCA) of the samples.

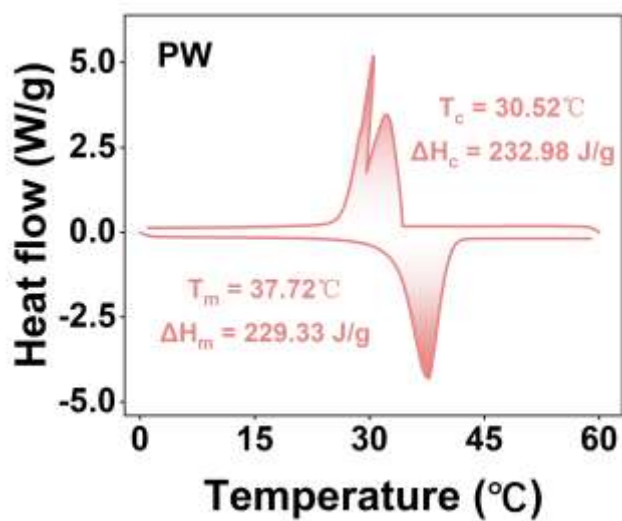


Figure S9 DSC curves of PW during melting and cooling.

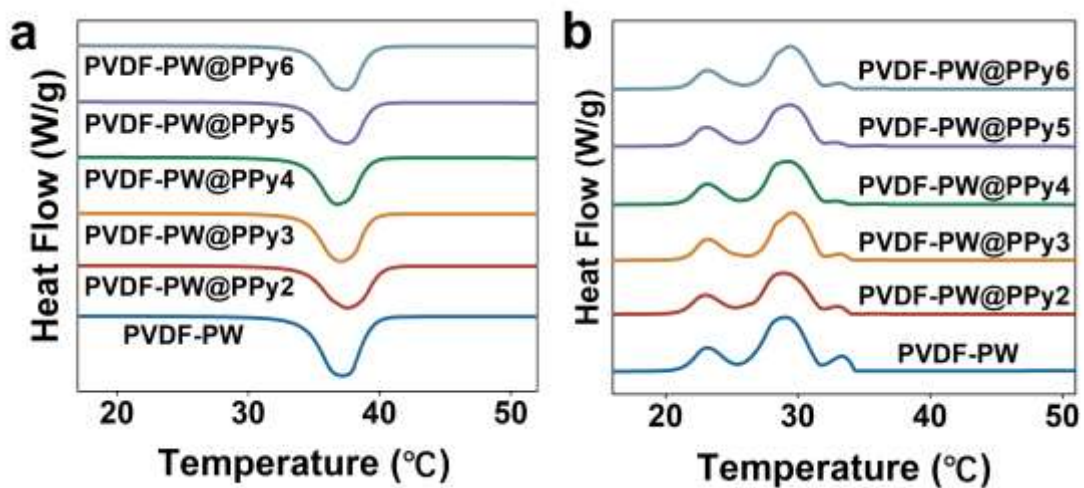


Figure S10 DSC curves of composite films during melting and cooling.

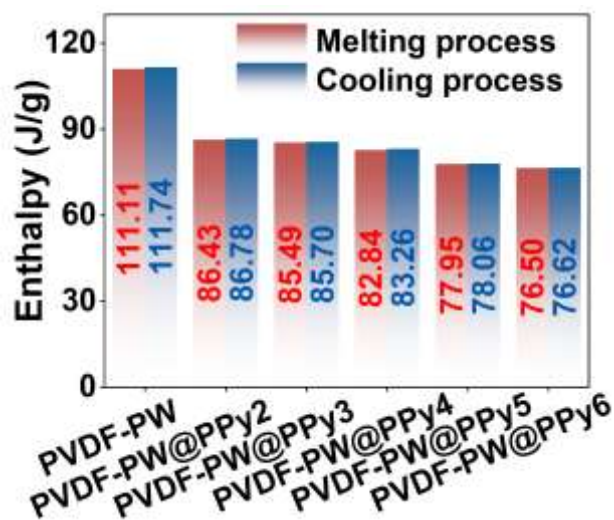


Figure S11 Phase change enthalpies of composite films.

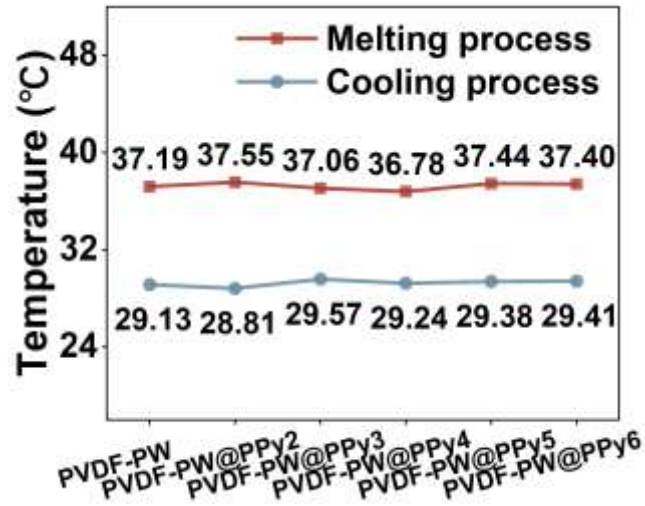


Figure S12 Phase change temperatures of composite films.

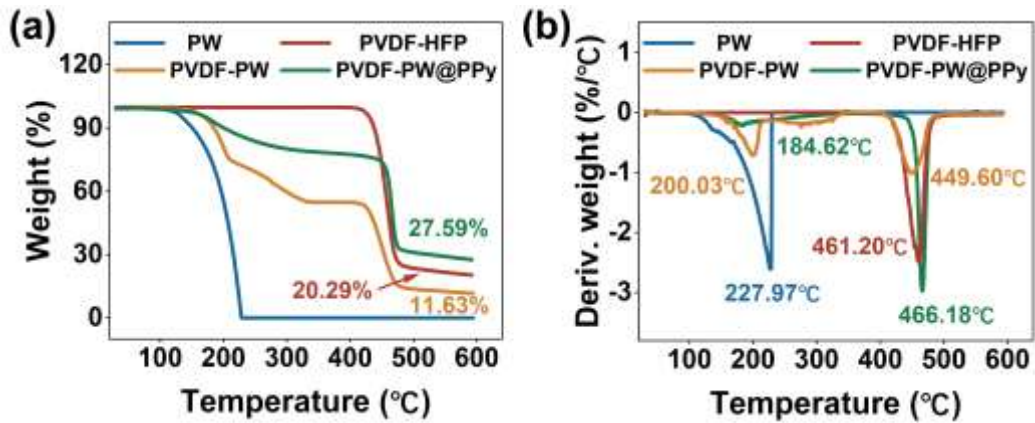


Figure S13 TG curves and DTG curves of the samples.

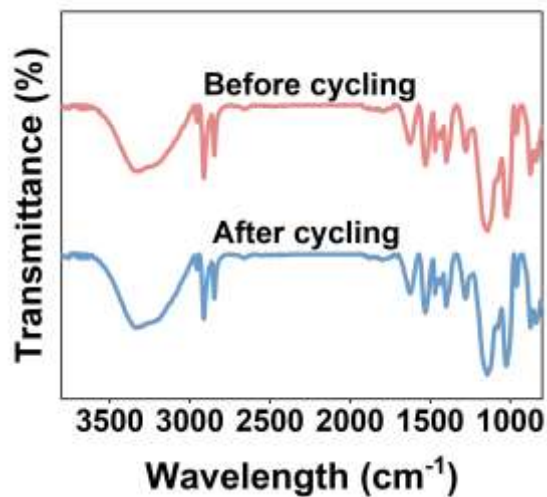


Figure S14 FT-IR curves before and after thermal cycling.

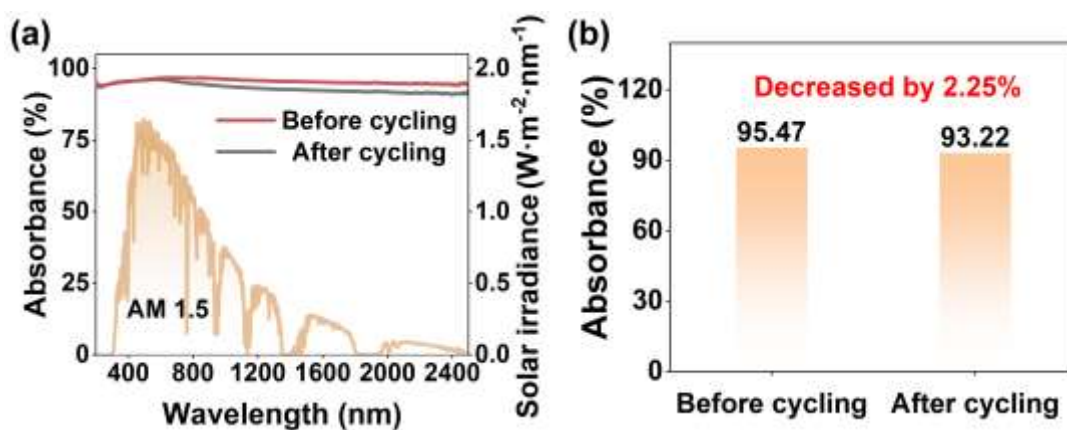


Figure S15 Absorbance of PVDF-PW@PPy composite film before and after 100 thermal cycling tests.

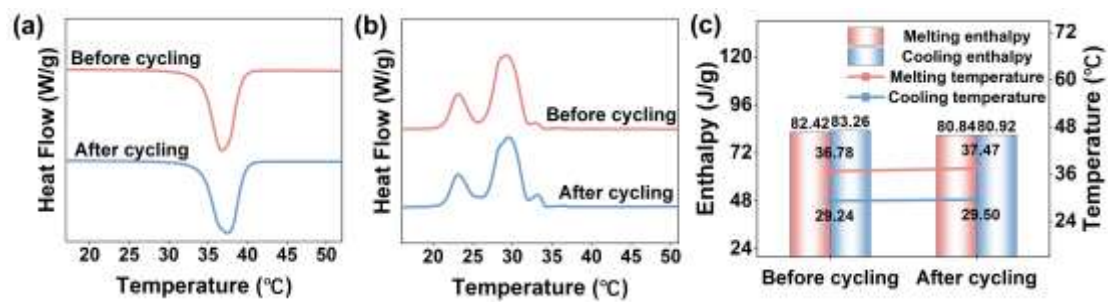


Figure S16 Phase change parameters before and after thermal cycling tests. (a) DSC curves during melting. (b) DSC curves during cooling. (c) Enthalpy values and phase change temperatures before and after testing.

Table S1 The relevant parameters of PVDF-PW@PPy composite films during solar-to-thermal conversion testing.

m (g)	ΔH_m (J/g)	P(W/cm ²)	S (cm ²)	t ₂ - t ₁ (s)	η (%)
0.42	82.43	0.06	2.72	-	-
0.52	81.91	0.07	2.56	383.23	62.02
0.55	80.76	0.08	2.56	325.97	66.54
0.44	82.84	0.09	2.40	212.87	79.27
0.47	80.76	0.10	2.72	148.54	93.95

Note: Where m is the mass of the composite film, g; ΔH_m is the enthalpy value during melting, J/g; P is the light intensity, W/cm²; S is the illuminated area, cm²; t₁ and t₂ are the starting and ending times of phase transition, s.